Int. J. Electrochem. Sci., 11 **(2016)** 10928 – 10938, doi: 10.20964/2016.12.81

International Journal of
ELECTROCHEMICAL
SCIENCE
www.electrochemsci.org

The Effects of Trace PbO on the Oxide Behavior of 304L Stainless Steel in High Temperature Water

Kexin LIANG, Yunfei XU, Wanwan WANG, Rongxue SHI, Yu TAN[*]*, Shenghan ZHANG*

School of Environment Science and Engineering, North China Electric Power University, Yonghua North Street 619, Baoding 071000, China
[*]E-mail: lucifertan@163.com

Received: 20 September 2016 / *Accepted:* 19 October 2016 / *Published:* 10 November 2016

304L stainless steel was corroded in a simulated PWR primary circuit at 315°C with ppb level PbO treatment. Corrosion properties and semiconductor behaviors of the oxide layers on SS304L exposed to high temperature and high pressure water corrosion were investigated by electrochemical potentiodynamic curves and Mott-Schottky tests. The FE-SEM images suggested some unprotective spinel crystals formed on the surface of oxide film with trace level PbO treatment. And XPS results indicated not only 2^+ valance but also 4^+ and 0 of Pb, cooperated with Iron, Chromium, Nickel and their oxides, in the oxide layer.

Keywords: High temperature and high pressure water; 304L stainless steels; PbO; Potentiodynamic curves; Mott-Schottky analysis

1. INTRODUCTION

Recently, nuclear power plants are highly developed for their clean energy property consideration [1]. With wide range of applications in nuclear power plant for construction material, 304L stainless steel (SS304L) plays an important role for its high corrosion resistance to the high temperature water environment. Fe-base alloy [2] forms a special oxide layer which indicated semiconductor behaviors in high temperature water (HTW). The semiconductor behaviors of this layer on metallic materials are highly interrelated to the corrosion activity, even with stress corrosion cracking [3]. The latest papers about stainless steel exposed to HTW mainly focused on the impact of concentration of hydrogen or oxygen [2, 4-7]. An outer sublayer with spinel oxide lattice by Fe enrichment of the oxide layer and an inner sublayer with Cr enrichment on stainless steel formed during the oxidation process in HTW with various chemical conditions [2, 8-11]. The metal ions,

which added or polluted into the high temperature water only very tiny amount of, may further modify the oxide film. Such as Zinc addition, which plays a positive role, has been studied for semiconductor properties [12-14] or mechanical properties [15-16] of Fe-based alloys. Zinc addition (also as Zinc injection, Zinc treatment), which indicates 5-25 ppb ZnO addition into the primary circuit of boiling water reactor (BWR) or pressurized water reactor (PWR) can restrain the ^{60}Co intrusion into the oxide films of Fe-based alloys and this technique has been adopted by 39 PWR until 2006 [17]. Nowadays, some articles [18-20] suggested pollution by PbO (lead oxide) indicated negative effect on the oxide layers on metallic materials in HTW environment. And some researchers studied stress corrosion cracking on metallic materials by PbO treatment for very high concentration as 500ppm [18, 21] or even higher as 10000ppm [22] which exceeded the 'real working condition' for water chemistry of nuclear power plant.

The mechanism that how the electrochemical properties or semiconductor behaviors changes is not clear by trace level PbO treatment into HTW. For this research, the oxide layers on SS304L formed with various trace concentration of PbO treatment (also with free ones) in neutral aqueous solution and electrochemical investigations were employed to study the changes of oxide layers by PbO treatment. And also, certain concentration of Co was employed in the solution to provide a real water chemistry condition of PWR.

2. MATERIALS AND METHOD

2.1. Materials composition and pretreatment

The materials used for this work is stainless steel 304L. The chemical compositions is shown as below (mass, %): 0.016 C, 0.66 Si, 1.66 Mn, 0.032 P, 0.005 S, 18.57 Cr, 10.39 Ni and balance Fe. Specimens (12mm×10mm×3mm) were mechanically ground up with SiC papers to 2000 grit and then mirror finished with 0.3μm alumina gel. Then specimens were, cleaned ultrasonically using ethanol and then pure water before oxidation process.

2.2. High temperature water corrosion

The HTW corrosion was carried out at 315°C, under 10.5 MPa in a 1L autoclave for 120h. The aqueous electrolyte contained 2ppm lithium hydroxide, 500ppm H_3BO_3 + $Na_2B_4O_7$ and 200ppb Co^{2+} with 10-100 ppb PbO and also a Pb-free contrast one. The as prepared samples are hanged in the autoclave and immersed into the solution. The solution in the autoclave was deareated continuously with pure N_2 for 2 hours before heating. After oxidation hours, the specimens were taken out for cleaning by flushing pure water and then stored in a dry box.

2.3. Surface analysis

After corrosion in HTW, the specimens were took out to ex-situ analyses to observe their morphology of the states of oxidized layers by field emission scanning electronic microscopy (FE-

SEM) and X-ray photoelectron spectroscopy (XPS), using Al monochromator with C 1s at 284.8eV and depth profiles analyzed by Ar^+ sputtering with a rate 30nm·min^{-1} according to the standard SiO_2.

2.4. Electrochemical measurements

A classical three-electrodes cell was used in the electrochemical experiments. A saturated calomel electrode (SCE) was used as the reference electrode and a platinum foil as the counter electrode. All electrochemical measurements are applied at room temperature. The electrolyte used in the measurements was 0.15mol·L^{-1} boric acid and 0.0375mol·L^{-1} sodium borate buffered solution (pH=8.4). Before test, high purified N_2 gas was bubbled for 2h to ensure the dissolved O2 concentration to a low level. The electrochemical measurements were applied using a PARSTAT2273 potentiostat. The polarization curves usually started from 0.2V less that the open circuit potential to the certain positive potential with a scanning rate of 1.0 mV·s^{-1}. The Mott-Schottky tests were applied from -1.0V to +1.0V (vs. SCE, the same below). This measurement was performed by step of 10mV in the negative direction superimposing sinusoidal perturbing amplitude 10mV with the frequency of 1000Hz.

3. RESULTS AND DISCUSSION

3.1. Morphology and composition of the oxide layer on SS304L with PbO treatment

The specimens still look shiny with metallic luster after taking out from the autoclave by exposure in HTW with various PbO treatments. Fig.1 indicated the morphologies of the oxide layers surface of SS304L after oxidation. The surfaces of SS304L oxidated in HTW condition without PbO treatment (as PbO-free one, Fig.1A, B) were covered by two types of oxide particles, sparsely larger oxide and densely smaller oxide. FOr 10ppb concentration of PbO treatment into HTW, the oxides on the film of SS304L changed to grow smaller oxides and cannot cover the original surface (Fig.1C, D). For 50ppb PbO treatment to HTW, a scaly corroded oxide film formed on SS304L specimen which means that the trace level PbO treatment into HTW may slow/stop the growing process of oxide layers on SS304L(Fig.1E, F). When the concentration of PbO rose to 100ppb, a large porous like corrosion production formed on the surface with small oxides which not covered the whole surface (Fig.1G, H). The SEM results indicated an impact by trace PbO to the oxide films on SS304L. It is believed that the oxide on stainless steel has the ability to protect the substrate in HTW. The irregular oxide involved by trace level treatment of PbO into HTW lowered the anti-corrosion ability of SS304L.

The depth profiles intensities of XPS (showed as weight %) of the oxide layers on SS304L corroded in HTW with 50ppb PbO treatment (b) and PbO-free one (a) are presented in Fig.2.

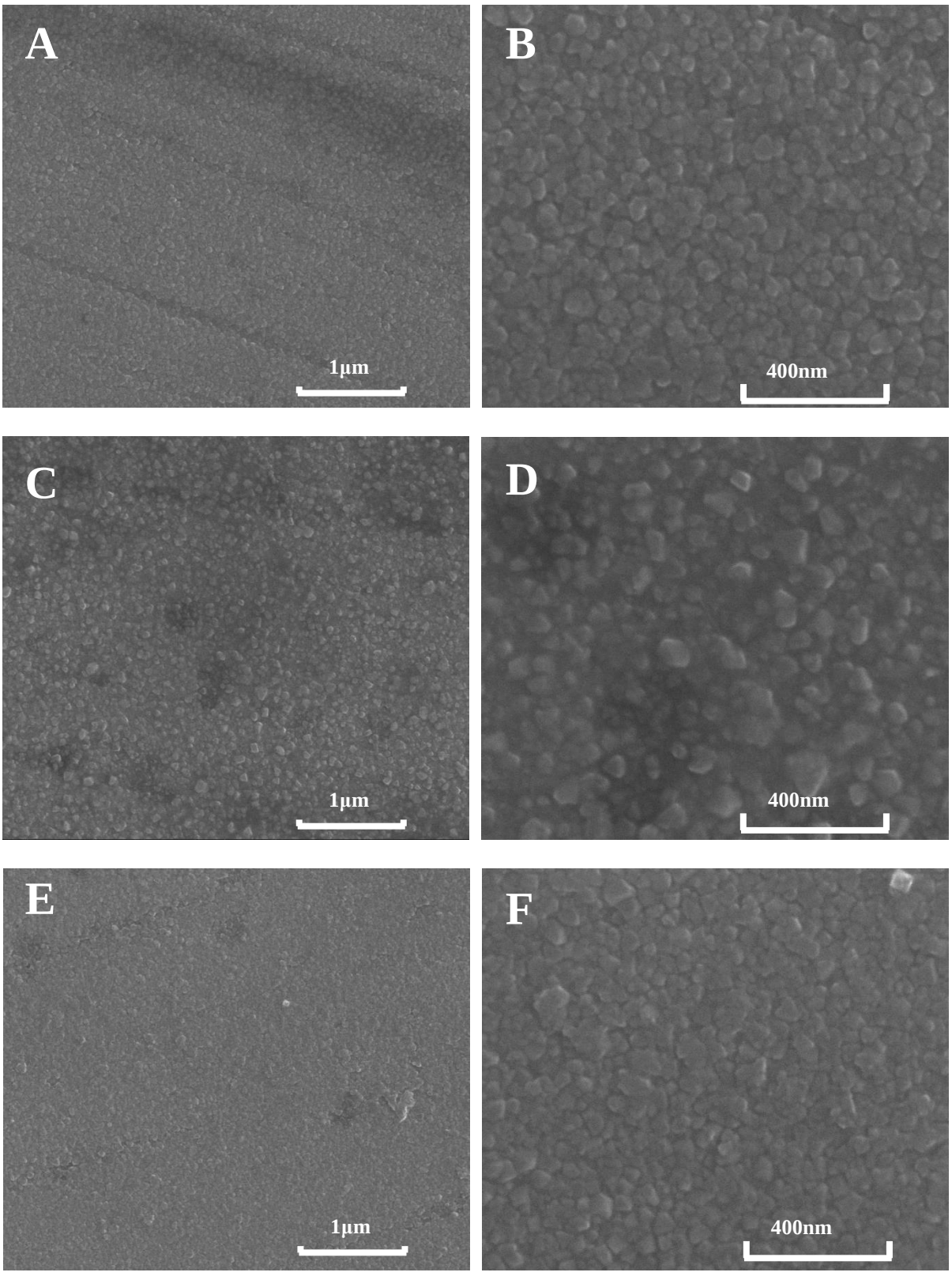
A
1μm
B
400nm
C
1μm
D
400nm
E
1μm
F
400nm

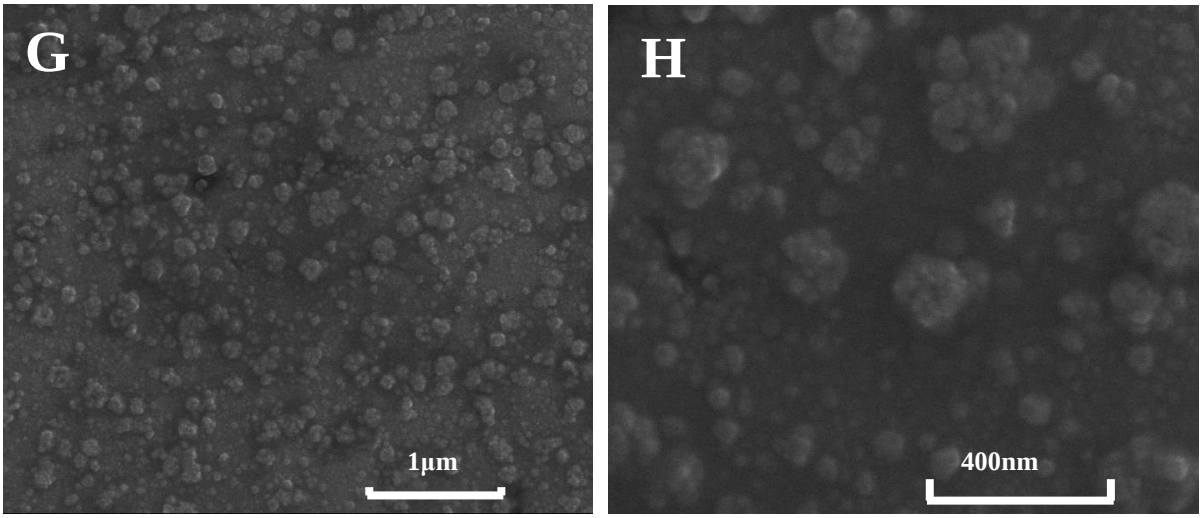

Figure 1. Morphology of the oxide layers on SS304L in HTW (A, B) without PbO treatment (PbO-free), (C, D) with 10ppb PbO, (E, F) with 50ppb PbO and (G, H) with 100ppb PbO treatment.

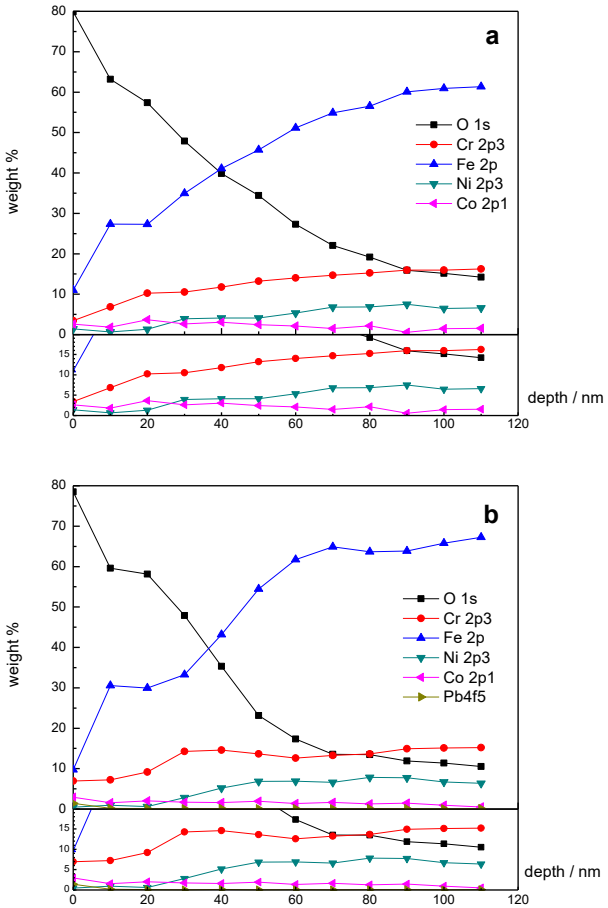

Figure 2. XPS depth profiles of SS304L corroded in HTW (a) without PbO treatment (PbO-free) and (b) with 50ppb PbO treatment.

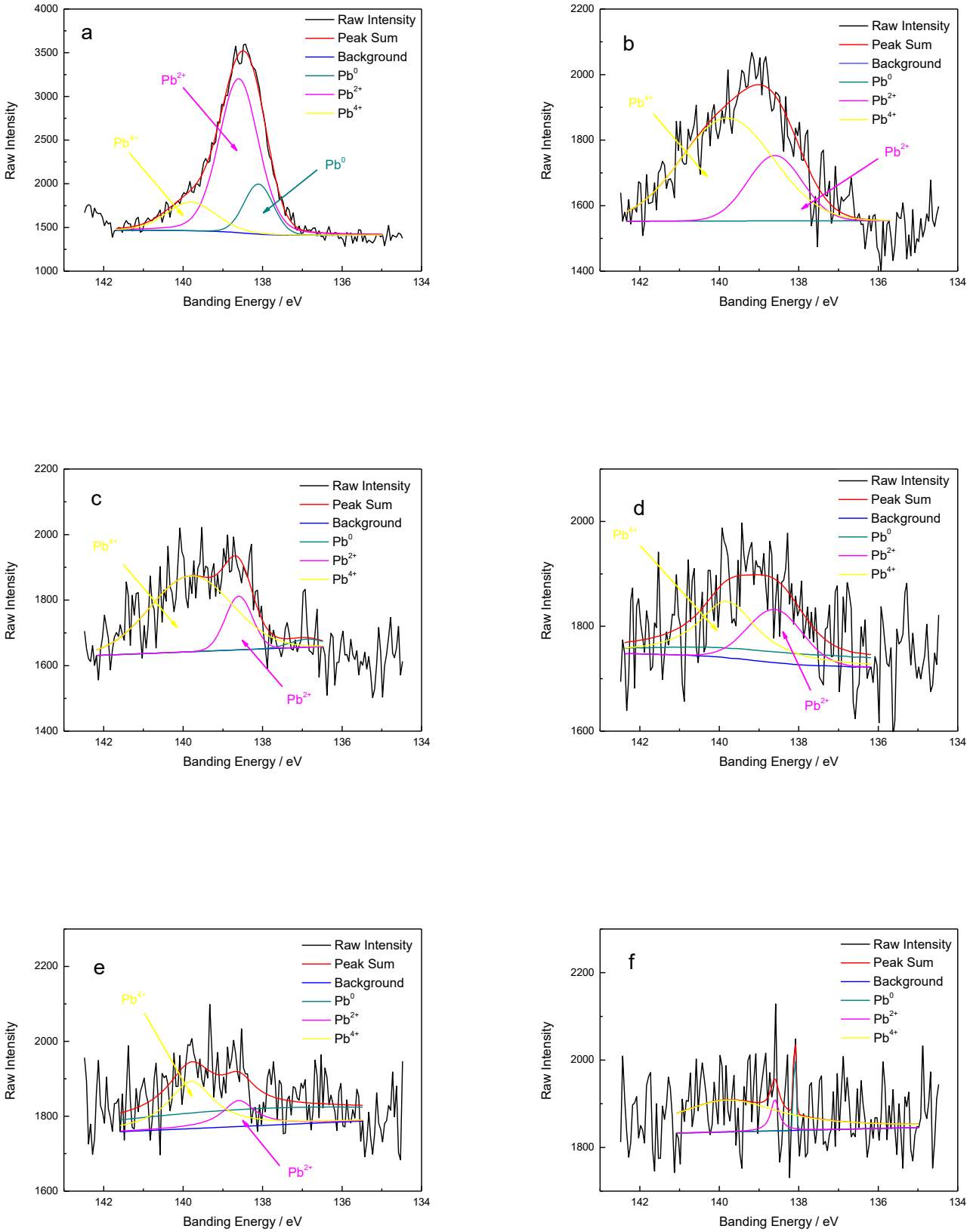

Figure 3. Detailed XPS fitting curves of Pb4f7/2 in the oxide layer on SS304L in HTW for different sputtering times.

It indicated a lower O(1s) concentration of oxide layer with PbO treatment as in Fig.2b rather than that of PbO-free on in Fig.2a. And also the concentrations of Cr and Ni are both lower than that of PbO-free one. This means the oxide film on SS304L with PbO treatment indicated less protective ability than that one without PbO. It should be highlighted that the concentration of Co decreases with PbO treatment into HTW. Co, doping in the oxide layer on alloys, may involve an occupational radiation exposure to the worker during the time window of maintenance. Though PbO treatment plays a positive effect on reduce Co, it also plays a disconfirming effect on the anti-corrosion behaviors of the SS304L in HTW.

A detailed xps fitting curves of concentration of Lead were shown as Fig.3 (a to f: from top to inner layer) which calculated from XPS results. It can be seen that an enrichment of Lead on the surface of the oxide layer on SS304L with 50ppb PbO treatment and both valance 0, +2 and +4 of Lead involved (as Fig.3a). This means that the PbO was not simple adhesion to the surface of the specimen but different valance states of Lead co-oxidated with other metallic materials such as Iron, Nickel and Chromium, besides Oxygen in the oxidation procedure. From a to f, the results indicated 10nm per depth as from the surface to inner layer. On the surface, the Pb^{2+} plays a main one because that Pb was added as PbO. From the surface to the inside, Pb^{4+} plays the main one rather than Pb^{2+} and seldom Pb^{0} can be seen (Fig.3b to e). It indicated no significant Pb (0, +2 or +4 valance) signals when reached the 50nm depth from the surface of the oxide layer(Fig.3f). The change of Pb^{2+} to Pb^{4+} in the oxide layer may cause a decrease of oxygen. And the co-worked Lead and Chromium may involve an unnormal decrease of Cr enrichment than the one without PbO treatment, which may cause the SCC of stainless steel.

And also X-ray diffraction (XRD) was employed in this experiment; the results were not typical and meaningful due to the very thin oxide film or small amount of Pb in the film. It is still not sure what the exact phase formed in the oxide layer on stainless steel corroded in HTW with PbO treatment.

3.2. Potentiodynamic polarization

The polarization curves of SS304L specimens corroded in HTW with various trace concentration of PbO treatment are plotted as Fig.4. The polarization curves of PbO-free one showed a classical curve as in a neutral electrolyte with passive state (E= 0.3~1.0V) and oxygen evolution reaction (E> 1.0V). The E_{corr} can be got from these curves. With 10ppb PbO treatment, the polarization plot indicated a positive movement of E_{corr}. And also, the polarization of oxide films formed with 50/100ppb treatment indicated the same trend but less positive movement. At the passive state, the plot with PbO treatment indicated a less average current i_{pass} than that without PbO, which may be caused by the co-oxidation of Pb and other metal oxide. From Fig.4, with an addition of PbO, the cathodic polarization current density increased while the anodic polarization current density decreased, obviously. Similar polarization curves have been reported for Alloy690 with a concentration of PbO 500ppm addition [22]. It means though the oxide layers on stainless steel corroded in HTW with PbO treatment is not so completed but the corrosion current in the potential dynamic test is lower.

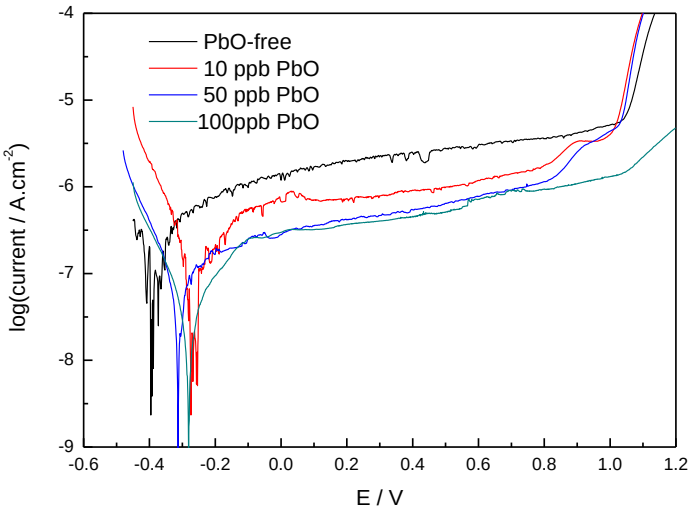

Figure 4. Potentiodynamic polarization curves of SS304L after HTW oxidation with different trace PbO treatment, at polarization rate of 1mV·s^{-1}.

3.3. Mott-Schottky Measurement

The Mott-Schottky measurement gives precise characteristics on semiconductor properties of the oxide films on alloys such as semiconductor type, density of donor (N_D) or acceptor (N_A) and flat band potential (E_{fb}). Fig.5 indicated the Mott-Schottky plots of the oxide layers on SS304L corroded in HTW with various PbO treatments.

According to the published papers [23-25], the oxide layers on alloys indicated different semiconductor behaviors. In this paper, when the electrode (metal) contact to the electrolyte, the oxide layer on electrode and the electrolyte indicated different charge. The excess charge layer is distributed in the space charge layer. When the space charge layer is in the depleted state, the capacity of the space charge layer plays a linear relationship with applied E as the below equation:

$$\frac{1}{C^2} = \frac{2}{\varepsilon\varepsilon_0 e N_D}\left(E - E_{fb} + \frac{KT}{e}\right) \quad (1)$$

Where ε indicates the dielectric constant of the oxide layer (15.6), ε_0 indicates the permittivity of free space (8.854×10^{-12} F·m^{-1}), e indicates the electron charge (1.602×10^{-19} C), K indicates the Boltzmann constant (1.38×10^{-23} J·K^{-1}) and T indicates the absolute temperature. For an n-type semiconductor, C^{-2} versus E should be linear with a positive slope that is inversely proportional to the donor density. In this paper, the positive slope, as an n-type semiconductor, was discussed for trace level PbO treatment into HTW. E_{fb} and N_D were discussed from the Mott-Schottky curves as Fig.5.

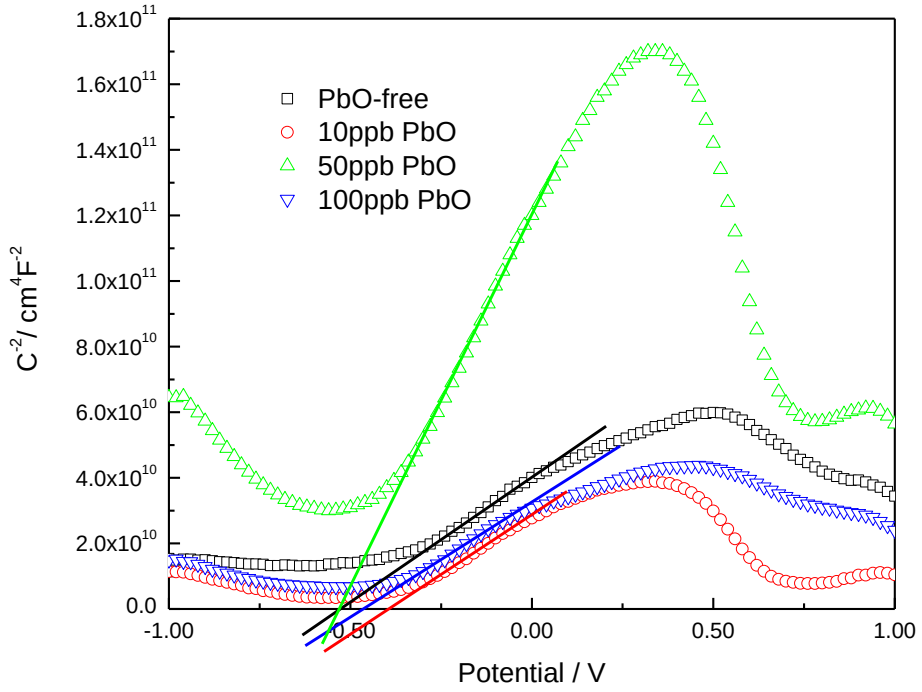

Figure 5. Mott-Schottky curves of oxide layers on SS304L corroded in HTW with various trace PbO treatment.

The as-calculated N_D was listed in Table.1, besides E_{fb}. With PbO treatment, E_{fb} of the oxide films on SS304L indicated a positive movement except that of the oxide layer with 50ppb PbO. And N_D shown a dramatic decreasing from 1.97($\times 10^{20} cm^{-3}$) to 0.586($\times 10^{20} cm^{-3}$) as concentration of PbO treatment increased from 0ppb to 50ppb. It indicated the same trend as the component analysis, the trace PbO treatment into HTW lower the oxidation process of Cr, Ni and others with dissolve O_2. It could be explained as that, during the oxidation process the PbO played a competition with Cr/Ni and also Co. So the concentration of Co in the oxide layer on SS 304L with PbO treatment is lower.

Table 1. E_{fb} and N_D calculated from Mott-Schottky curves of oxide layers on SS304L after HTW oxidation with various trace PbO treatments.

PbO addition (ppb)	$N_D(\times 10^{20}\ cm^{-3})$	E_{fb}(V)
0	1.97	-0.52
10	1.91	-0.45
50	0.586	-0.54
100	2.10	-0.37

These results of the semiconductor behaviors of oxide layer on SS304L can also give some explanations about the potentiodynamic polarization plots of that as Fig.4. When the potentiodynamic

polarization test proceeded, the one with smaller N_D indicated a smaller average corrosion current. When the treatment of PbO turned to 100ppb, the N_D indicated an enhancement than that with 0, 10 or 50ppb treatment. It probably caused a water chemistry condition deterioration and the oxide film on SS304L totally turned into porous.

4. CONCLUSIONS

We reported an oxide layer on SS304L corroded in HTW with ppb level PbO treatment. The corrosion current of oxide layer formed with PbO treatment shown reduction than the PbO-free one. The capacities tests show n-type semiconductors of oxide layer on SS304L after corrosion with/without PbO treatment and the donor density of the oxide films decreases by property PbO treatment. The trace level PbO treatment into HTW stopped the oxide surface layer to form spinel metallic oxides.

ACKNOWLEDGEMENTS
The work is supported by 'the Fundamental Research Funds for the Central Universities'.

References

1. Long-term development plan of nuclear power (2011-2020), the National Development and Reform Commission, October 2012.
2. S. E. Ziemniak, M. Hanson and P. C. Sander, *Corros. Sci.*, 50 (2008) 2465.
3. R. B. Rebak and Z. Szklarska-Smialowska, *Corros. Sci.*, 38 (1996) 971.
4. D. Rodriguez and D. Chidambaram, *Appl. Surf. Sci.*, 347 (2015) 10.
5. H. C. Wu, B. Yang and S. L. Wang, *Mater. Sci. Eng.*, A, 633 (2015) 176.
6. K. Wang, J. Wang and W. Hu, *Mater. Des.*, 82 (2015) 155.
7. T. Massoud, V. Maurice, L. H. Klein, A. Seyeux and P. Marcus, *Corros. Sci.*, 84 (2014) 198.
8. W. Kuang, X. Wu and E.-H. Han, *Corros. Sci.*, 69 (2013) 197.
9. Y. Qiu, T. Shoji and Z. Lu, *Corros. Sci.*, 53 (2011) 1983.
10. V. S. Sathyaseelan, A. L. Rufus ,P. Chandramohan, H. Subramanian, T. V. K. Mohan, S. V. Narasimhan and S. Velmurugan, *Prog. Nucl. Energ.*, 59 (2012) 100.
11. S. Zhang, L. Jia and T. Yu, *Electrochim. Acta*, 89 (2013) 253.
12. S. Zhang, Y. Tan and K. Liang, *Mater. Lett.*, 68 (2012) 36.
13. X. Liu, X. Wu and E.-H. Han, *Corros. Sci.*, 65 (2012) 136.
14. J. Huang, X. Liu, E.-H. Han and X. Wu, *Corros. Sci.*, 53 (2011) 3254.
15. S. E. Ziemniak and M. Hanson, *Corros. Sci.*, 48 (2006) 2525.
16. S. E. Ziemniak and M. Hanson, *Corros. Sci.*, 48 (2006) 3330.
17. Peter Andresen, Meeting Between the Nuclear Regulatory Commission (NRC) Staff, Industry Representatives, and Electric Power Research Institute/Materials Reliability Project Representatives on Mitigation of Primary Water Stress Corrosion Cracking, NRC headquarters in Rockville, Maryland, May 30, 2007.
18. S. S. Hwang, U. C. Kim and Y. S. Park, *J. Nucl. Mater.*, 246 (1997) 77.
19. A. Palani, B. T. Lu, L. P. Tian, J. L. Luo and Y. C. Lu, *J. Nucl. Mater.*, 396 (2010) 189.
20. S. S. Hwang, H. P. Kim, Y. S. Lim, J. S. Kim and L. Thomas, *Corros. Sci.*, 49 (2007) 3797.
21. S. Ahn, V. Shankar Rao, H. Kwon and U. Kim, *Corros. Sci.*, 48 (2006) 1137.

22. D.-J. Kim, H. C. Kwon, H. W. Kim, S. S. Hwang and H. P. Kim, *Corros. Sci.*, 53 (2011) 1247.
23. W. Li and J. Luo, *Electrochem. Commun.*, 1 (1999) 349.
24. A. Di Paola, D. Shukla and U. Stimming, *Electrochim. Acta*, 36 (1991) 345.
25. C. Sunseri, S. Piazza and F. Di Quarto, *J. Electrochem. Soc.*, 137 (1990) 2411.
26. D. D. Macdonald, *J. Electrochem. Soc.*, 139 (1992) 3434.